RAA 2016 Vol. **16** No. **9**, 144 (6pp) doi: 10.1088/1674–4527/16/9/144
http://www.raa-journal.org *http://iopscience.iop.org/raa*

***R**esearch in*
***A**stronomy and*
***A**strophysics*

A sodium laser guide star coupling efficiency measurement method

Lu Feng[1], Zhi-Xia Shen[1], Suijian Xue[1], Yang-Peng Li[1], Kai Jin[2], Angel Otarola[4], Yong Bo[3], Jun-Wei Zuo[3], Qi Bian[3], Kai Wei[2] and Jing-Yao Hu[1]

[1] Key Laboratory of Optical Astronomy, National Astronomical Observatories, Chinese Academy of Sciences, Beijing 100012, China; *jacobfeng@bao.ac.cn*
[2] The Institute of Optics and Electronics, Chinese Academy of Sciences, Chengdu 610209, China
[3] Technical Institute of Physics and Chemistry, Chinese Academy of Sciences, Beijing 100190, China
[4] Thirty Meter Telescope Corporation, Pasadena, California, USA

Received 2016 April 15; accepted 2016 May 18

Abstract A large telescope's adaptive optics (AO) system requires one or more bright artificial laser guide stars to improve its sky coverage. The recent advent of a high power sodium laser is perfect for such application. However, besides the output power, other parameters of the laser also have a significant impact on the brightness of the generated sodium laser guide star, mostly in non-linear relationships. When tuning and optimizing these parameters it is necessary to tune based on a laser guide star generation performance metric. Although return photon fluxis widely used, variability of the atmosphere and sodium layer makes it difficult to compare results from different sites or even within a short time period for the same site. A new metric, coupling efficiency, is adopted in our field tests. In this paper, we will introduce our method for measuring the coupling efficiency of a 20W class pulse sodium laser for AO application during field tests that were conducted during 2013–2015.

Key words: instrumentation: adaptive optics — methods: observational — atmospheric effects

1 INTRODUCTION

Adaptive optics (AO) is one of the latest technologies that has significantly improved the performance of large ground-based astronomical telescopes in terms of image sharpness and sensitivity. The operation of the system relies strongly on the detection performance of the turbulence induced aberrated wavefront which comes from a bright on-sky reference source that should be within an isotropic angle from the observed target (Hardy 1998). The sky coverage of such bright stars is reported to be less than 1% in the near infrared band (Ellerbroek & Tyler 1998), which severely limits the application of an AO system. The introduction of artificial laser guide star technology alleviates this problem. By projecting a suitably designed laser close to the direction of the observed target, one could generate an artificial guide star in the sky that will lower the requirement of the brightness of a natural guide star, thus improving the sky coverage of the AO system. There are two methods used in generating a laser guide star; one is taking advantage of Rayleigh backscatter induced by light scattered by large molecules and dust in the lower atmosphere (0∼20 km), the other is by exciting sodium atoms in the high atmosphere (90∼110 km) with a sodium laser and using the resonant fluorescence of these sodium atoms as the reference signal. Because the sodium laser guide star has a higher altitude, which is beneficial for sensing a larger volume of turbulence than the Rayleigh laser guide star, it is preferable for generating a laser guide star.

The brightness of the sodium laser guide star has a direct impact on the wavefront detection performance of the AO system. A pulsed laser when combined with the range-gating technique, could avoid the "fratricide effect" which is caused by Rayleigh backscatter in the lower atmosphere. The first generation sodium pulse lasers had an output power merely at the level of a few watts. However, it was soon found that by further increasing the output power or reducing the pulse width, the return flux would be easily saturated. Theoretical modeling (Holzlöhner et al. 2010a,b; Rampy et al. 2012) showed that it is necessary to tune the laser's temporal/spectral behavior as well as other characteristic parameters to take advantage of the physics of the sodium atom to further increase the return flux. An optimum set of parameters for the laser has to be determined with an on-sky test based on a certain metric which should be able to reflect the absolute performance of the laser during laser guide star generation. In earlier papers, the metric used was often reported to be return photon flux measured by differential photometry with a Johnson V band filter. This metric is fine for tuning if the duration of the test is short compared to the variability of sodium abundance. However, it is possible that the sodium abundance in the atmosphere can change from 2×10^{13} to more than 10×10^{13}atoms m^{-2} in one night (Pfrommer et al. 2009),

and it could be even higher in a short time interval due to a sporadic pocket of sodium concentration in the atmosphere. A new metric was used in Holzloehner's paper about an AO simulation (Holzlöhner et al. 2010a), the coupling efficiency of the sodium laser, which was formerly used in the Lidar equation. We repeat the Lidar equation here in Equation (1). The coupling efficiency of the laser $s_{\rm ce}$ is on the left side. On the right side, the return flux in unit receiver area F (unit photons $\rm s^{-1}$ $\rm m^{-2}$) is normalized with laser power in the mesosphere $P(T_{\rm a})^X$, the sodium column abundance $C_{\rm Na}$ and considering the airmass X and the height of the sodium layer L.

$$s_{\rm ce} = \frac{FL^2}{P(T_{\rm a})^{2X} C_{\rm Na} X}. \quad (1)$$

The coupling efficiency thus has the advantage that it is invariant with respect to changes in sodium abundance, sodium layer height, atmospheric transparency, and laser power variations if all parameters in the equation could be measured synchronously at the same location. The complexity and cost of the measurement system hinders the popularity of this metric. However, because it directly reflects the absolute performance of the laser in generating a laser guide star, it is the most helpful metric for optimizing the internal parameters of a sodium laser in the field or comparing with numerical simulations. Since 2011, we have developed and improved our measurement method for this parameter and thoroughly used this method in field tests of our prototype lasers. In this paper, we will introduce our measurement method and present a comparison of the results between one of our latest field tests using this method and the simulation.

2 SITE PREPARATION AND EQUIPMENT SETUP

As mentioned in Equation (1), several parameters have to be measured simultaneously to determine the coupling efficiency of the laser. These parameters and related measurement equipment used during our field tests are listed in Table 1.

The left panel of Figure 1 shows our setup used during the 2015 Xinglong test campaign (Feng 2015; **?**). Similar layouts were adopted in our previous tests with minor changes to accommodate space constraints (Gaomeigu 2013 test, Jin et al. 2014, Gaomeigu 2014 test, Jin et al. 2015, UBC 2013 test in Vancouver, Canada, Otarola et al. 2016). The LGS laser and the sodium Lidar laser were located in a modified clean room in a laboratory building on the site. Two hatches were installed on the laboratory ceiling right above the Laser Launching Telescope (LLT) of the LGS laser and the zenith pointing fold mirror of the Lidar laser respectively for launching lasers to the zenith. A make-shift shelter was built 20 meters away from laser launching points. The choice of its location was limited by the surrounding buildings and terrain, but it was decided that it should not be too far away from the launching points to minimize LGS spot elongation and synchronous delay for Lidar. The shelter also had two hatches installed on its roof. The 32 cm LGS photometry telescope and a 50 cm Dobsonian telescope for the Lidar system were set up under these hatches respectively. A 25 cm auxiliary telescope provided by the Xinglong site was used routinely during test nights to monitor the atmospheric transmission.

A schematic diagram of the LGS laser beam transfer optics is shown in the right panel of Figure 1. The 589.159 nm sodium laser comes out from the port side of the package. The combination of the half-wave plate and the thin-film polarizer acts as power attenuator for adjusting projected laser power. An Electro Optics Modulator (EOM) is used to generate the sodium $\rm D2_{\it b}$ line sidebands from the original $\rm D2_{\it a}$ line for the $\rm D2_{\it b}$ repumping technique which will enhance the photon flux return (Kibblewhite 2009). A Quarter-Wave Plate (QWP) is added after the EOM to adjust the polarization of the output laser beam. A pair of lenses is inserted to adjust the laser beam width to fully fill the input aperture of the LLT. A large space is intentionally left between the 1st and 2nd fold mirrors after the beam expander. This space is for switching asynchronous parameter measurement setups, for instance, setups for measuring beam width, pointing, polarization, pulse shape, spectrum, etc. These measurements are done intermittently every night because most of these parameters are stable once settled. If one of these parameters is not stable, it can be observed by instability of wavelength or power, which are constantly monitored by a monitor stage inside the laser package. A tiny fraction of the 589 nm laser inside the laser package is guided to this stage. A wavelength monitor and a power meter are mounted and kept monitoring while the laser is on.

3 OBSERVATION AND DATA REDUCTION

Observations using the laser guide star are only conducted on cloudless nights. The procedure for laser guide star observation is summarized in Figure 2. Before every observation, the LGS laser has to be re-optimized to have the maximum stable power output, as well as a stable wavelength near 589.159nm ($\rm D2_{\it a}$ line). The LGS photometry telescope pointing to the zenith is refocused with natural stars. The LGS laser is then projected to the zenith. Because the laser beam has a Gaussian profile, it is necessary to refocus the beam to the sodium layer by adjusting the focal length of the launching telescope (Fig. 2(a)). The LGS return flux profile versus wavelength is determined by the emission line of the sodium atom and the Doppler broadening effect. The profile shows that the highest return flux happens when the laser is tuned to the $\rm D2_{\it a}$ line of the sodium atom (Steck 2010). The wavelength of the LGS laser is thus optimized by maximizing the return flux of the LGS (Fig. 2(b)). It has been reported (Kibblewhite 2009; Holzlöhner et al. 2010a) that polarization of the laser beam could affect the pumping efficiency of the sodium laser, thereby affecting the return flux of the LGS. The circular polarization has the highest return flux, while the linear polarization has the lowest. Although it is possible to measure the beam's polarization on the bench (right panel of Fig. 1), we choose to determine polarization by return

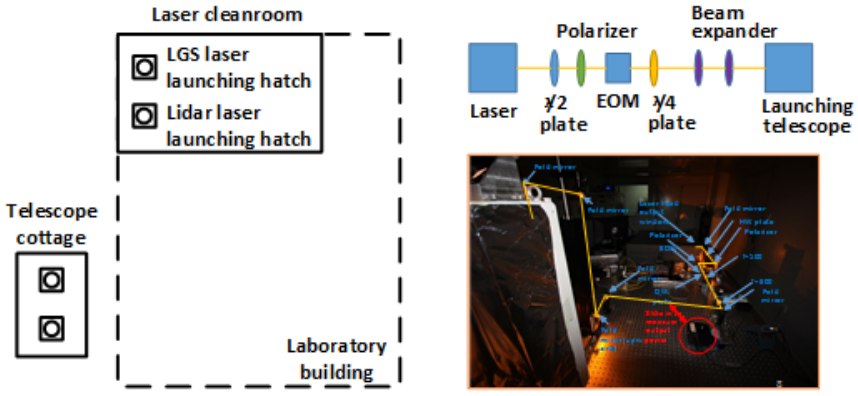

Fig. 1 (*Left*) Schematic diagram of the LGS coupling efficiency measurement facility for the Xinglong test campaign. A similar design was also utilized for previous field tests. (*Upper right*) Schematic diagram of the beam transfer optics for the LGS laser. (*Lower right*) Actual layout of the laser bench. The red circle marks where equipment used for asynchronous laser parameter measurement can be switched in/out.

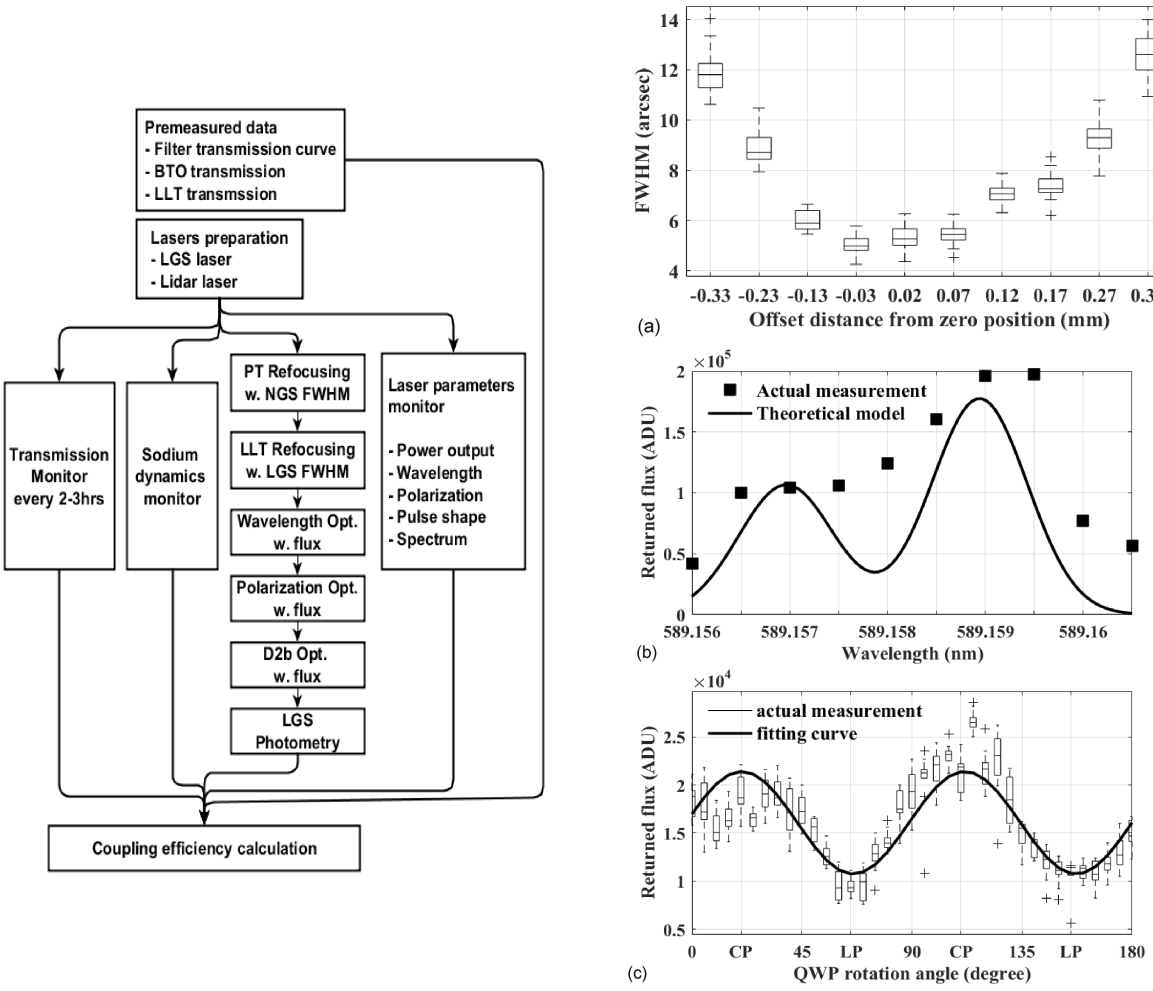

Fig. 2 (*Left*) Laser guide star coupling efficiency measurement procedure. (*Right*) Parameter tuning before coupling efficiency measurement: (a) LLT focal stage tuning versus LGS FWHM, (b) wavelength tuning versus LGS return flux, (c) polarization tuning versus LGS return flux.

Table 1 Equipment for measuring parameters in the Lidar equation

Parameter name	Measurement equipment	Description
return flux of laser guide star (F)	photometry telescope	Planewave 12.5 inch Corrected Dall-Kirkham telescope
	Johnson V band filter	Standard Johnson UBVRI filter
	CCD camera	Princeton Instruments 512×512 electrically cooled camera
sodium column density ($C_{\rm Na}$) and sodium layer centroid height (L)	sodium Lidar	CSSC sodium Lidar
laser power (P)	power meter	ThorLabs PM100D with S120C sensor
atmospheric transmission ($T_{\rm a}$)	auxiliary telescope	25 cm telescope

flux because there are several reflecting surfaces after the test point that could alter the final polarization. The polarization optimization is done by adjusting the rotation angle of the QWP to where the return flux has the highest value (Fig. 2(c)). By controlling the modulation depth of the EOM, the amount of power shifted from D2$_a$ to D2$_b$ is controlled. This fraction is optimized to around 10-15% of the total laser power (Holzlöhner et al. 2010a; Rampy et al. 2012; Feng et al. 2015).

While the sodium laser guide star is in operation, we also keep monitoring the temporal variance of the sodium layer's column density $C_{\rm Na}$ as well as its central height L with the sodium Lidar. The atmospheric transmission $T_{\rm a}$ is monitored every 2–3 hours by the 25 cm telescope.

We chose a Johnson V-band filter because it is easy to acquire and relatively cheap. However, because the filter's spectral range is much wider than the Doppler broadened spectral width of the sodium atom, the application of this filter introduces two disadvantages for photometry of the sodium laser guide star:

- Contamination from other wavelengths within the filter band reduces photometry precision;
- V magnitude of the natural star is calculated by integrating all lights within the filter band because the star's spectrum is wider than the filter bandwidth. Integrating LGS light within this band and comparing with the star's V magnitude will decrease the value of actual brightness of the LGS.

The first disadvantage is trivial for us because the magnitude of the laser guide star we generated is in the range of $v7$ to $v7.5$, and sky background noise is trivial compared to the laser guide star's brightness. To solve the second problem introduced by the mismatch between the filter band and the narrow band of sodium fluorescence, we resort to the natural reference star's spectrum rather than the V magnitude value that was previously used for differential photometry. However, because the photometry telescope is pointing to the zenith, there is one more complication in that during field tests we have to identify stars in LGS images that already have their spectra measured and logged in publicly accessible databases of large spectral surveys, such as the LAMOST DR3 database (Cui 2015).

The photometry of the LGS star is thus done by the following. The reference natural star and the laser guide star from the image are extracted. The coordinates of the natural star are then identified (Lang et al. 2010). We search the spectrum $F(\lambda)$ of the star by its coordinates in the LAMOST DR3 database. If the star's spectrum can be found in the database, its spectrum along with its V magnitude will be used to calculate the LGS's photon flux. A normalized photon flux of the star in the V band is then calculated with,

$$F_V = \frac{1}{hc}\int_0^\infty F(\lambda)W(\lambda)\lambda d\lambda, \tag{2}$$

where $W(\lambda)$ is the V band response function (multiplication of the V band filter transmission curve and quantum efficiency curve of the CCD). Since we know that at $\lambda_0 = 555.6\,{\rm nm}$ for the A0 star Vega, the value of $F_{\lambda_0}^{\rm Vega}$ is $9.4\times10^7\,{\rm s^{-1}\,m^{-2}\,nm^{-1}}$. Therefore, the normalized photon flux from the reference star, at λ_0, could be calculated by,

$$F_\lambda(\lambda_0) = 10^{-0.4V}\frac{F_{0V}^{\rm Vega}}{F_{0V}}F_\lambda^{\rm Vega}(\lambda_0). \tag{3}$$

The absolute photon flux from the reference star at any wavelength λ could then be found by,

$$F_\lambda(\lambda) = \frac{\lambda F_\lambda(\lambda)}{\lambda_0 F_\lambda(\lambda_0)}F_\lambda(\lambda_0). \tag{4}$$

The instrumental flux measured by the CCD, in ADC units, is given by,

$$F_{\rm inst} = A\int_0^\infty F_\lambda W(\lambda)d\lambda, \tag{5}$$

where conversion factor A is a proportionality constant related to the telescope area, throughput, CCD gain and atmospheric transmission which does not vary over a short time scale. Therefore, with an identified star in the image, we could calculate A by Equation (5) and apply this value in Equation (6) to calculate the absolute photon flux of the laser guide star.

$$F_{\rm LGS} = \frac{F_{\rm LGSinst}}{AW(589.159\,{\rm nm})}, \tag{6}$$

where $F_{\rm LGSinst}$ is the laser guide star's instrumental flux in the unit of ADU measured from the CCD. The coupling efficiency can be calculated by Equation (1) after $F_{\rm LGS}$ is determined.

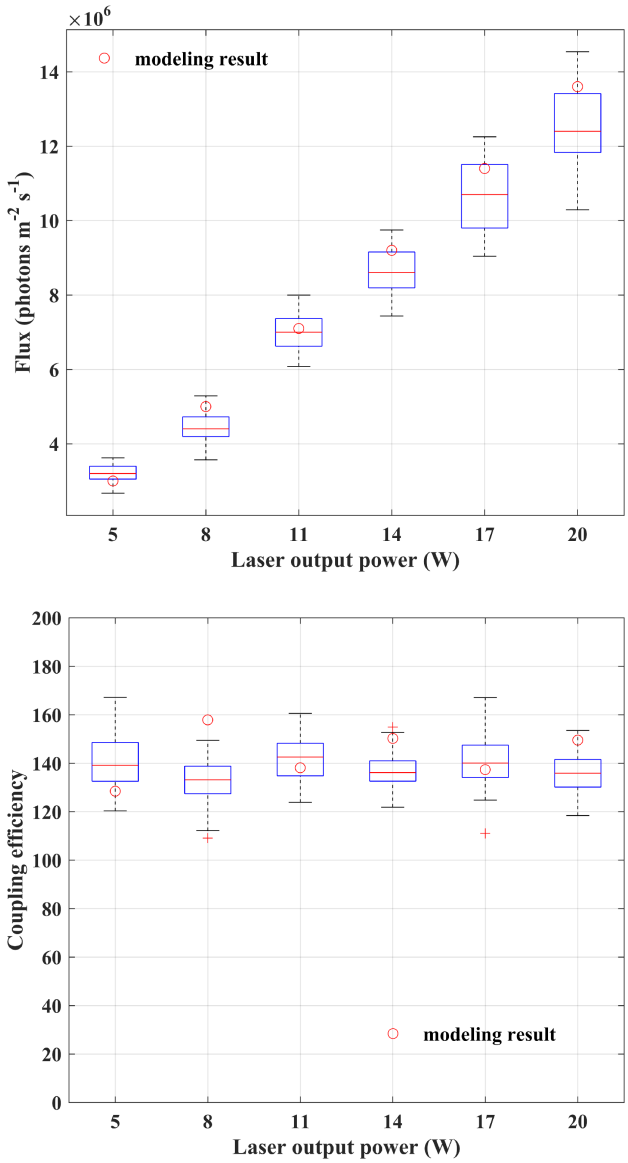

Fig. 3 Comparison between measurement results and modeling results. Each box in the boxplot contains 30 images of the actual measurements.

In Figure 3, we showed measured results of LGS flux and coupling efficiency measured with the method described during one night of our 2015 Xinglong test campaign. The laser was working at 800 Hz, circular polarization with a 120 ns pulse width and a 10% power branching ratio for $D2_b$ repumping. A simulation was conducted with real-time measurement data such as laser spectrum, pulse profile, polarization state, laser direction, sodium column density as well as sodium layer height. Results from the simulation are also plotted against the measurements which show a good agreement between theoretical modeling and the measurement with this method.

4 CONCLUSIONS

In this paper, we showed a new method for measuring the performance of a sodium laser in the generation of LGS. A new metric, the coupling efficiency of the laser which reflects the absolute performance for LGS generation, is used instead of the flux of LGS. A test setup for the measurement as well as the calculation method using LAMOST spectral data to calibrate the filter effect is described. Coupling efficiency measurement results are compared with simulation results, and a good agreement is presented.

Acknowledgements This work was supported by the National Natural Science Foundation of China (11303056 and 11273002), the NAOC astronomical financial special fund (Y533061V01), and Key Laboratory of Optical Astronomy, CAS. We acknowledge help from Xinglong and Gaomeigu Observatories. We greatly appreciate help from Prof. Wang Ji-Hong and Prof. Yang Guo-Tao from the National Space Science Center for their sodium Lidar support, and Dr. Jia Ming-Jiao from University of Science and Technology of China for his support in Lidar raw data analysis.

References

Cui, X. 2015, Data Release 3 of the Lamost Spectral Survey (*http://dr3.lamost.org*)

Ellerbroek, B. L., & Tyler, D. W. 1998, PASP, 110, 165

Feng, L. 2015, IAU General Assembly, 22, 2254336

Feng, L., Kibblewhite, E., Jin, K., et al. 2015, in Proc. SPIE, 9678, AOPC 2015: Telescope and Space Optical Instrumentation, 96781B

Hardy, J. W. 1998, Adaptive Optics for Astronomical Telescopes (Oxford University Press), 448

Holzlöhner, R., Rochester, S. M., Bonaccini Calia, D., et al. 2010a, A&A, 510, A20

Holzlöhner, R., Rochester, S. M., Pfrommer, T., et al. 2010b, in Proc. SPIE, 7736, Adaptive Optics Systems II, 77360V

Jin, K., Wei, K., Xie, S., et al. 2014, in Proc. SPIE, 9148, Adaptive Optics Systems IV, 91483L

Jin, K., Wei, K., Feng, L., et al. 2015, PASP, 127, 749

Kibblewhite, E. 2009, in Advanced Maui Optical and Space Surveillance Technologies Conference, E33

Lang, D., Hogg, D. W., Mierle, K., Blanton, M., & Roweis, S. 2010, AJ, 139, 1782

Otarola, A., Hickson, P., Gagne, R., et al. 2016, Journal of Astronomical Instrumentation, 1650001, in press

Pfrommer, T., Hickson, P., & She, C.-Y. 2009, Geophys. Res. Lett., 36, L15831

Rampy, R., Gavel, D., Rochester, S., & Holzlöhner, R. 2012, in Proc. SPIE, 8447, Adaptive Optics Systems III, 84474L

Steck, D. 2010, Sodium D Line Data, available at *http://steck.us/alkalidata*